
not-so-BigGAN: Generating High-Fidelity Images on a Small Compute Budget

Seungwook Han*
MIT-IBM Watson AI Lab
IBM Research
seungwook.han@ibm.com

Akash Srivastava*
MIT-IBM Watson AI Lab
IBM Research
akash.srivastava@ibm.com

Cole Hurwitz*
MIT-IBM Watson AI Lab
University of Edinburgh
cole.hurwitz@ed.ac.uk

Prasanna Sattigeri
IBM Research
psattig@us.ibm.com

David D. Cox
MIT-IBM Watson AI Lab
IBM Research
david.d.cox@ibm.com

Abstract

BigGAN is the state-of-the-art in high-resolution image generation, successfully leveraging advancements in scalable computing and theoretical understanding of generative adversarial methods to set new records in conditional image generation. A major part of BigGAN’s success is due to its use of large mini-batch sizes during training in high dimensions. While effective, this technique requires an incredible amount of compute resources and/or time (256 TPU-v3 Cores), putting the model out of reach for the larger research community. In this paper, we present NOT-SO-BIGGAN, a simple and scalable framework for training deep generative models on high-dimensional natural images. Instead of modelling the image in pixel space like in BigGAN, NOT-SO-BIGGAN uses wavelet transformations to bypass the curse of dimensionality, reducing the overall compute requirement significantly. Through extensive empirical evaluation, we demonstrate that for a fixed compute budget, NOT-SO-BIGGAN converges several times faster than BigGAN, reaching competitive image quality with an order of magnitude lower compute budget (4 Tesla-V100 GPUs).

1 Introduction

Generative modelling of natural images has achieved great success in recent years [15, 9, 3, 18, 33]. With advancements in scalable computing and theoretical understanding of generative models [21, 33, 10, 19, 20, 27, 22, 30, 31], state-of-the-art techniques are able to not only generate photo-realistic images but also scale to higher dimensions than ever before [5, 24].

At the forefront of high-resolution image generation is BigGAN [5], a generative adversarial network (GAN) [9] that meets the curse of dimensionality (CoD) head-on using the latest in scalable GPU-computing. This allows for training BigGAN with large mini-batch sizes (e.g., 2048) that greatly helps to model high-dimensional, complex datasets such as Imagenet. As such, BigGAN’s ability to scale to high-dimensional data, comes at the cost of a hefty compute budget. A standard BigGAN model can require a few weeks of training time on as many as eight Tesla V100 graphics processing units (GPUs). This compute requirement raises the barrier to entry for using and improving upon these technologies as the wider research community may not have access to any specialized hardware (e.g., Tensor processing units (TPUs) [14]). The environmental impact of training large-scale models can also be substantial as training BigGAN on 512x512 pixel images for just two days reportedly

*equal contribution

used as much electricity as the average American household does in about six months (when using 512 TPUs) [29].

Motivated by these concerns, we present NOT-SO-BIGGAN, a small compute alternative to BigGAN for class-conditional modelling of high-resolution images. NOT-SO-BIGGAN completely bypasses the CoD by applying wavelet transformation to the data, decomposing the high-dimensional images into several sets of low-dimensional images [11, 7, 2]. When applied to a 2D image, WT slices the image into four equally-sized image-like patches along different frequency bands. This process can be recursively applied multiple times in order to slice a large image into multiple smaller images, each one representing the entire image in different bandwidths. This is diagrammatically shown in Figure 1. Here, the top-left patch (TL) lies in the lowest frequency band and contains most of the structure of the original image. The highly sparse top-right (TR), bottom-left (BL) and bottom-right (BR) patches lie in higher bands of frequency.

NOT-SO-BIGGAN uses a deterministic encoder that recursively applies WT to the input image, retaining only the low frequency TL patch as a lossy, compressed representation of input. This technique is conceptually similar to image compression methods, such as JPEG2000 [2], which is in fact based on WT. NOT-SO-BIGGAN’s decoder then uses this TL patch to learn how to reconstruct the missing TR, BL and BR patches. Once all the patches are reconstructed, the input image can be recovered using IWT. Since NOT-SO-BIGGAN’s deterministic encoder leads to an *image-like* latent space that is made up of low-dimensional TL patches, it is easy to sample from this space by training a smaller generative model. This is referred to as learning the prior [24]. For this step, we train a BigGAN-based sampler on the low-dimensional latent space. Since this BigGAN-based sampler only has to learn to generate low-dimensional TL patches rather than the full resolution image, it has significantly lower compute requirements and training time. Please refer to Figure 2 for a visual summary of NOT-SO-BIGGAN.

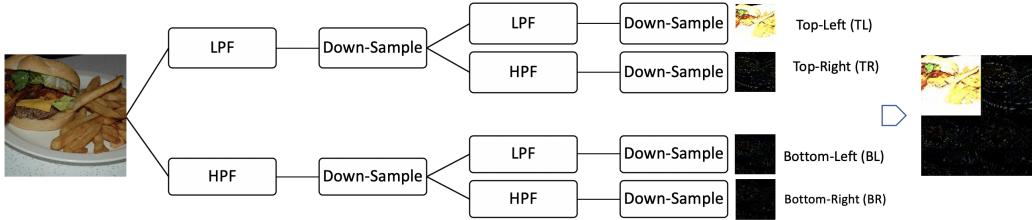


Figure 1: Wavelet transformation consists of a low-pass and a high-pass filter, followed by a down-sampling step that splits the image into two equal-sized patches. Each of these two patches undergo the same operation again resulting in four equal-sized patches, TL, TR, BL and BR.

2 Background

Given a set $X = \{x_i | \forall i \in \{1, \dots, N\}, x_i \in \mathbb{R}^D\}$ of samples from the true data distribution $p(x)$, the task of deep generative modelling is to approximate this distribution using deep neural-networks. All generative models of natural images assume that $p(x)$ is supported on a K -dimensional, smaller manifold of \mathbb{R}^D . As such, they model the data using a conditional distribution $p_\theta(x|z)$, where θ represents the model parameters and $Z \in \mathbb{R}^K$ is the latent variable with the prior $p(z)$. Z is marginalized to obtain the log-likelihood (LLH) $\log p_\theta(x) = \log \int p(z) p_\theta(x|z) dz$ of X under the model. Generative model are trained by either maximising this LLH or its lower-bound.

There are two types of deep generative models, explicit models like variational autoencoders (VAE) [15] that have an explicit form for the LLH and implicit models such as GANs [9] that do not have such a form. VAEs use a decoder network D_θ to parameterize the model distribution $p_\theta(x|z)$ and an encoder network E_ϕ to parameterize a variational distribution $q_\phi(z|x)$ as an approximation to the true posterior under the model. They can then be trained using the evidence lower-bound (ELBO),

$$\log p_\theta(x) \geq -\text{KL}[q_\phi(z|x)||p(z)] + \int q_\phi(z|x) \log p_\theta(x|z) dz. \quad (1)$$

KL here refers to the Kullback–Leibler divergence between $q_\phi(z|x)$ and $p(z)$. Unlike VAEs, GANs do not make any assumptions about the functional form of the conditional distribution $p_\theta(x|z)$ and,

therefore, do not have a tractable likelihood function. Instead, they directly attempt to minimize either a variational lowerbound to a chosen f -divergence [22, 30] or integral probability metric (IPM) [3, 17, 31] between the model distribution $p_\theta(x)$ and $p(x)$. This is achieved by pitching the decoder network D_θ against a neural network-based binary classifier C_ω . C_ω is trained to distinguish between samples from $p(x)$ and samples from D_θ while D_θ is trained to fool C_ω . The solution of this saddle-point problem leads D_θ to produce samples that are indistinguishable from the true data. In practice, saddle point optimisation is a challenging problem that suffers with increasing data dimensionality.

Wavelet Transform. Wavelet transformation of an image (illustrated in Figure 1) is a two-step recursive process that splits the original image into four equal-sized patches, each a representation of the entire image in different frequency bands. In the first step, a low-pass filter (LPF) and a high pass-filter (HPF) are applied to the original image. This produces two patches of the same size as the original image. Since the application of LPF and HPF leads to redundancy, we can apply Shannon-Nyquist theorem to downsample these patches by half without losing any information. In step two, the same process is repeated on the output of step one, splitting the original image into four equally-sized patches (TL, TR, BL and BR). TR, BL and BR contain increasingly higher frequencies of the input image, preserving horizontal, vertical and diagonal edge information, respectively (contributing to the sharpness of the image).

3 Related Work

While not directly targeted at lowering the compute requirements for BigGAN, there has been a considerable amount of work in improving likelihood-based generative models for high-resolution image generation. VQVAE-2 [24] is the state-of-the-art, achieving the highest image quality for an autoregressive model with an explicit likelihood function. VQVAE-2 is a hierarchical version of the VQVAE model [23]. It uses the same vector quantization technique from VQVAE to learn a hierarchical discrete representation of image. Unlike other variational autoencoding-based models, VQVAE-2 does not impose a KL-based regularisation on the latent space and instead uses vector quantization as a strong functional prior. As such, sampling from the latent space is not straightforward. In fact, a large part of VQVAE-2 training budget is spent on training several auto-regressive PixelSNAIL [6] models to estimate the density on the latent space of the model. The training of these autoregressive samplers is slow and cannot be parallelized, resulting in a fairly high overall train time.

Our method is closely related to the Subscale Pixel Network (SPN) [18] and multi-scale model of [25]. [18] shows that it is easier to generate high resolution images by splitting the process into two steps. In step one, they slice the image into small patches and then learn to generate these patches using a patch-level autoregressive model. This step allows for capturing the general structure of the image but misses the finer details. Therefore, in step two, they train another network that learns to fill in the missing details. The SPN model has a significant shortcoming, however, as its patch-level autoregressive approach fails to capture long term dependencies (e.g. eyes on a face looking in different directions). Similar to SPN’s multi-scale approach, NOT-SO-BIGGAN decouples structure learning from adding details. Unlike SPN, however, it does not suffer from the long-term dependency problem. This is because NOT-SO-BIGGAN uses wavelet transformation to slice the image, which naturally decouples the structure (TL) from the details (TR, BL, BR) in the image. We demonstrate this difference diagrammatically in the Appendix A. More importantly, wavelet transform alleviates the need for autoregressive modelling of the patches as each patch represents the entire image in different frequency bands. The fact that we can learn to construct these patches altogether – not sequentially – drastically speeds up the overall training.

Another line of work that closely relates to NOT-SO-BIGGAN is *super-resolution* (SR), where a deep network is trained to up-sample a low-resolution input image so as to restore the loss in sharpness and details. Compared to NOT-SO-BIGGAN, the state-of-art SR models [16, 32], operate in the full dimensionality of the target image and therefore, have higher compute requirements and similar training instability issues as BigGAN. As we will show, using wavelet based up-sampling of our method is not only efficient, it also leads to better sample quality compared to a pixel-based SR method.

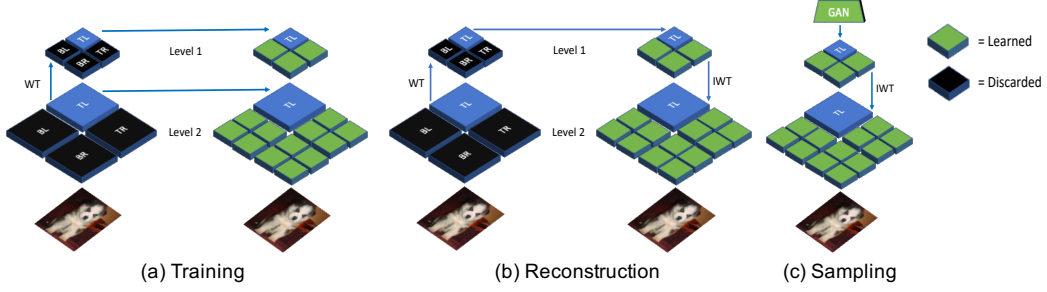


Figure 2: NOT-SO-BIGGAN schematic for (a) training, (b) reconstruction and (c) sampling.

4 Method

NOT-SO-BIGGAN is best described as an autoencoder that operates in the frequency domain instead of the usual pixel space. It is comprised of a deterministic encoder, a partly-learned decoder, and learned prior network. These three components form a full generative model that can produce high-quality, high-resolution samples with under a week of training on commodity hardware.

4.1 Deterministic Encoder

The NOT-SO-BIGGAN encoder is a deterministic function that recursively applies a wavelet transform to the input image, *retaining only the TL patches at each level*. Each TL patch is a quarter of the size of the previous TL patch, resulting in a pyramid-like stack of 2D patches after multiple transformations. Since TL contains the lowest frequencies and, therefore, the most structural information about the image, we use it as a compressed, lossy representation of the input image in our encoding step.

For a N^2 -dimensional image X , let us denote the matrix obtained after wavelet transform as $W(X)$, which is a $N \times N$ block matrix with the following structure,

$$W(X) = \begin{bmatrix} W_{1,1}(X) & W_{1,2}(X) \\ W_{2,1}(X) & W_{2,2}(X) \end{bmatrix}.$$

Here, with a slight abuse of notation, $W_{1,1}(X)$ represents the $(\frac{N}{2} \times \frac{N}{2})$ -dimensional TL patch of image X . NOT-SO-BIGGAN’s encoder \mathcal{E} can then be defined recursively as follows,

$$\begin{aligned} \mathcal{E}_0(X) &= X \\ \mathcal{E}_l(X) &= W_{1,1}(\mathcal{E}_{l-1}(X)), \quad 1 \leq l \leq L \end{aligned} \quad (2)$$

where l is the number of wavelet transforms applied to the input image. As can be seen, the size of the retained TL patch decreases exponentially with l .

4.2 Decoder

After a wavelet transform, the original image can be deterministically recovered from the TL, TR, BL, and BR patches using IWT. NOT-SO-BIGGAN, however, discards the high-frequency patches during its encoding step, rendering a fully deterministic decoding impossible. To resolve this, the NOT-SO-BIGGAN decoder is realized as a combination of a learned and a deterministic function that first learns to recover the missing high-frequency patches (using a neural network) and then deterministically combine them using IWT to reconstruct the original input.

Since NOT-SO-BIGGAN’s encoding operation recursively applies wavelet transforms and discards the high-frequency components at each of the L encoding levels, we train L decoder networks to reconstruct the missing frequencies at each corresponding level of decoding. To parallelize the training of these decoder networks, we perform multiple wavelet transforms to the original high-resolution dataset, generating L training sets of TL, TR, BL and BR patches. This allows us to independently train each of the decoder networks (in a supervised manner) to reconstruct the missing high-frequency patches conditioned on the corresponding TL. This parallelisation boosts the convergence rate of NOT-SO-BIGGAN, allowing for a fully trained decoder in under 48 hours.

Again with a slight abuse of notation, let $W_{1,1}^l$ be the TL patch at level l and $\text{IWT} = \text{WT}^{-1}$. We can write the decoder for level l as

$$D_l(W_{1,1}^l; \Theta) = \text{IWT} \left(\left[\begin{array}{c|c} W_{1,1}^l & f_{\theta_{1,2}}^l(W_{1,1}^l) \\ \hline f_{\theta_{2,1}}^l(W_{1,1}^l) & f_{\theta_{2,2}}^l(W_{1,1}^l) \end{array} \right] \right) \\ \text{for } 1 \leq l \leq L. \quad (3)$$

Here, each f^l is a deep neural network that is trained to reconstruct one of the TR, BL, or BR patches at level l , conditioned on the TL patch ($W_{1,1}^l$).

The main challenge in high-resolution image generation lies in overcoming the curse of dimensionality. But by leveraging IWT, the original dimensionality of the image is completely bypassed in the NOT-SO-BIGGAN decoder. Therefore, in practice, at each level, we further divide the TR, BL and BR patches by applying WT until we reach the patch dimensionality of 32x32. This can be done irrespective of the original dimensionality of the image. We then reconstruct these patches in parallel and recover the patches and the original image by recursively applying IWT. This ability of NOT-SO-BIGGAN to bypass the original dimensionality of the input separates it from all other SR methods that operate in the pixel space.

Architecture: We realize each of the L decoder neural networks f_{θ_l} with a slightly modified version of the UNet architecture [26] rather than the commonly used transposed-convolution based architecture. UNet is typically used for image segmentation and object detection tasks. As shown in Figure 6 in the Appendix, UNet is an autoencoder architecture that has skip-connections from each encoding layer to its corresponding decoding layer. These skip connections copy and paste the encoding layer’s output into the decoding layer, allowing the decoder to exclusively focus on reconstructing only the missing, residual information. This architectural design makes it a compelling fit for decoding in NOT-SO-BIGGAN. We modify the UNet architecture by appending three shallow networks to its output with each one reconstructing one of the three high-frequency patches. This setup allows us to capture the dependencies between the high-frequency patches while also allowing sufficient capacity to capture to their individual differences.

4.3 Learned Prior Network

While we do not place any distributional prior on the latent space, the functional prior, in the form of a deterministic WT, leads to a highly structured representation space made up of low frequency TL patches of images. In order to generate from NOT-SO-BIGGAN, one must be able to draw sample from this space. We posit that, compared to sampling from equivalently-sized representation spaces for AE and VAEs, it is easier to sample from a low-dimensional, image-like latent space using generative methods such as GANs, as they repeatedly have been shown to excel in learning to samples from image distributions. Therefore, we train a BigGAN sampler on this representation space. The low-dimensionality of the TL patches allows us to train the BigGAN sampler without using large mini-batch sizes. Thereby, we are able train it using only two GPUs and with a single week of compute.

4.4 Training

As before, let X be the dataset of high-dimensional natural images. The NOT-SO-BIGGAN encoder can be defined as a deterministic function $\mathcal{E} : \mathbb{R}^D \mapsto \mathbb{R}^K$ that uses the WT to produce $Z = \{z_j | \forall j \in \{1, \dots, N\}, z_j \in \mathbb{R}^K\}$. Using this paired dataset $\{X, Z\}$, we treat NOT-SO-BIGGAN as a fully observable model and train the decoder function $D_\theta : \mathbb{R}^K \mapsto \mathbb{R}^D$ to reconstruct X from Z by minimising the negative log-likelihood (NLL) $-\mathbb{E}_{p(x,z)}[\log p_\theta(x|z)]$ of the conditional probability distribution that it parameterizes.

Learning of the generator function $G_\phi : \mathbb{R}^K \mapsto \mathbb{R}^K$ which is referred to as *learning the prior* in previous literature [24, 8], is essentially fitting a generative model to the marginal distribution of Z , i.e. $p(z)$. While we could use a similar approach as above and fit G_ϕ that parameterizes the model distribution $p_\phi(z)$ by minimising $-\mathbb{E}_{p(z)}[\log p_\phi(z)]$, we chose to instead use a BigGAN model to directly minimize the (variational lower-bound to the) f -divergence $\mathbb{D}_f[p(z) || p_\phi(z)]$ [22] between the true marginal distribution $p(z)$ and the model distribution as it provides a better fit for natural-image like distributions compared to other approaches.

All together, NOT-SO-BIGGAN simply specifies a generative model over X and Z jointly and is, therefore, trained by minimising the NLL,

$$-\mathbb{E}_{p(x,z)}[\log p_{\theta,\phi}(x,z)] = -\mathbb{E}_{p(x,z)}[\log p_{\theta}(x|z)] - \mathbb{E}_{p(z)}[\log p_{\phi}(z)]. \quad (4)$$

4.5 NOT-SO-BIGGAN-PIXEL

The NOT-SO-BIGGAN encoder works in the wavelet space, deterministically removing high-frequency components to generate a low-resolution, image-like latent representation. It is also possible, however, to encode a low-resolution, image-like representation by *directly sub-sampling the original image in pixel space* using an interpolation-based image-scaling method. This leads us to NOT-SO-BIGGAN-PIXEL, a pixel-space realisation of our method. As mentioned already, the encoding process for NOT-SO-BIGGAN-PIXEL consists of applying an interpolation-based down-sampling method to the original image. In this case, the latent space of NOT-SO-BIGGAN-PIXEL is a low-resolution version of the original image. While the encoding process in both NOT-SO-BIGGAN and NOT-SO-BIGGAN-PIXEL closely resemble each-other, their decoding processes are distinct.

The NOT-SO-BIGGAN-PIXEL decoder is also a partly-learned function that uses a modified UNet-based architecture. First, the encoded image is deterministically upsampled using an interpolation-based method. As shown in Figure 7a in the Appendix, this leads to a low-quality, blurry image of the same size as the original image. We then train a UNet to fill in the missing details in a similar approach to image super-resolution methods [13]. Unlike the NOT-SO-BIGGAN decoder that circumvents the CoD by avoiding reconstructions in the original data dimensionality, the NOT-SO-BIGGAN-PIXEL decoder still has to operate on the full image size, resulting in a larger decoder.

5 Experiments

In this section, we quantitatively and qualitatively evaluate our proposed models, benchmarking them against BigGAN on both image quality and training efficiency. While quantifying image quality remains an unsolved problem [4], we report the Frechet Inception Distance (FID) [12] and Inception Score (IS) [28] as proxy measures to allow for straightforward comparison with BigGAN.

Compute Budget. We train all the models for a total of 168 hours (7 full days). Our training is performed on a single machine with four V100 Tesla cards that have 16GB of VRAM each. We chose this hardware configuration for our experiments as it is a low-budget setup that is commonly used in deep learning research. Both of our models utilize a BigGAN-based sampler which comes in two different architectures, BigGAN-deep and BigGAN. Since the training of these BigGAN-based samplers are highly unstable [34], we train 5 instances in total (3 BigGAN-deep and 2 BigGAN samplers) and report results using the instance with the best FID/IS score.

Hyperparameters and Setup. For the deterministic encoder using wavelet transformation, we instantiate it with biorthogonal 2.2 wavelet. We use three sets of hyperparameters for training the three components of NOT-SO-BIGGAN. One set of hyperparameters is used for the sampler of NOT-SO-BIGGAN, another for the first-level decoder of NOT-SO-BIGGAN, and another for the second-level decoder of NOT-SO-BIGGAN. For the NOT-SO-BIGGAN sampler, we use a batch size of 512 and learning rates of 10^{-4} and 4×10^{-4} for the generator and discriminator, respectively. For the first-level decoder, we use a batch size of 128 and a learning rate of 10^{-4} . For the second-level decoder, we use the same learning rate as the first-level decoder, but a smaller batch size of 64. We allocate two GPUs to the NOT-SO-BIGGAN sampler, one GPU to the first-level decoder, and one GPU to the second-level decoder during training. Each component is trained in parallel and independently from each other. To train the BigGAN baseline model at the native resolution of 256×256 , we use the same learning rates as for the NOT-SO-BIGGAN sampler and a recommended batch size of 2048 [5]. The baseline model trains with eight GPUs, instead of four like with NOT-SO-BIGGAN, to meet its large memory requirement, given the batch size and resolution of the image. We provide training and evaluation code for NOT-SO-BIGGAN sampler and the other models, respectively here: <https://anonymous.4open.science/r/ca7a3f2e-5c27-48bd-a3bc-2dceadc138c1/>.

Truncation Trick The BigGAN model can trade off sample diversity for image fidelity using the "truncation trick" [5]. This trick consists of reducing the variance of the sampling noise distribution (truncation level) which improves IS and worsens FID. For this reason, we evaluate each model with

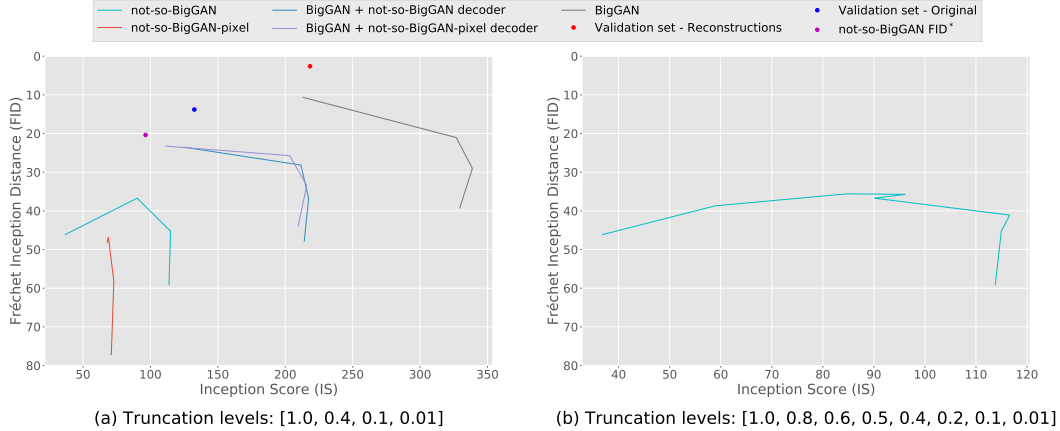


Figure 3: NOT-SO-BIGGAN FID/IS score.

four different levels of truncation, [1.0, 0.4, 0.1, 0.01]. To further explore the effect of the truncation trick on the NOT-SO-BIGGAN model, we evaluate NOT-SO-BIGGAN with finer-grained truncation levels: [1.0, 0.8, 0.6, 0.5, 0.4, 0.2, 0.1, 0.01].

5.1 Results

As shown in Figure 3(a), NOT-SO-BIGGAN attains the highest FID score of ~ 46 without truncation by the end of day 7 (as compared to NOT-SO-BIGGAN-PIXEL and the BigGAN model baseline). For reference, a fully-trained VQVAE-2 model achieves an FID of ~ 41 without truncation but at an order of magnitude higher compute budget of 128 TPU-v3 cores running for 140 hours. We also find that for both NOT-SO-BIGGAN and NOT-SO-BIGGAN-PIXEL, the FID decreases and IS increases with higher truncation levels, as expected. NOT-SO-BIGGAN is able to achieve a much better FID score of ~ 35 for a truncation level of 0.6, as shown in Figure 3(b).

[24] points out that FID and IS are sensitive to noise in the reconstructions. Following their example, we also measure the FID and IS between the generated samples and the reconstructions. Similar to VQVAE-2, NOT-SO-BIGGAN samples have a significantly lower FID of ~ 20 with respect to the reconstruction dataset as shown by the NOT-SO-BIGGAN FID* marker. Unfortunately, all three instances of the BigGAN baseline models diverged early in the training without ever crossing an FID of 250. Moreover, the BigGAN baseline models require a large batch size (2048) of 256×256 -dimensional images. Even with eight GPUs, we could only fit 64 images and its gradients. Therefore, as implemented in the official PyTorch version of BigGAN, we accumulated gradients over 32 mini-batches. We observed that this computation overhead heavily penalizes training speed and convergence. We find a similar divergence problem with the training of the BigGAN-deep sampler for the NOT-SO-BIGGAN-PIXEL model, where all three instances diverged at an FID of ~ 50 . However, by switching to the BigGAN sampler, we were eventually able to get two out of the three instances to converge. Interestingly, all instances of the NOT-SO-BIGGAN sampler, for both BigGAN and BigGAN-deep, were stable and converged without any issues.

Convergence. The decoders for both of our models quickly converge within 24-48 hours of training. It is highly likely, however, that our BigGAN-based samplers require more than 7 days of training before fully converging. To approximate the performance of our model with a fully converged sampler, we use the official pre-trained BigGAN at 256×256 [1]. This is possible because we can transform samples/reconstructions from the BigGAN model into NOT-SO-BIGGAN’s latent space using NOT-SO-BIGGAN’s deterministic encoder. The green and red curves in Figure 3 suggest that our models could potentially achieve much higher FIDs if the samplers are trained for longer. We would like to acknowledge, however, that this is an imperfect approximation of NOT-SO-BIGGAN’s best possible performance and that actually training our samplers *in the latent space directly* for longer may lead to better or worse results.

Decoder Generalisation. The NOT-SO-BIGGAN decoder is not only memory efficient and fast to train but also generalizes well to the validation dataset, as demonstrated by the small difference

	Train MSE	Validation MSE
NOT-SO-BIGGAN	0.0045	0.0049
VQVAE-2	0.0047	0.0050
NOT-SO-BIGGAN-PIXEL	0.0061	0.0074

Table 1: MSE on training and validation set for NOT-SO-BIGGAN, VQVAE-2 and NOT-SO-BIGGAN-PIXEL models. Small difference between the training and validation error suggests that both the models generalize well.

(0.0004) in the training and validation error in Table 1. The NOT-SO-BIGGAN decoder also reaches a lower MSE error than that of the VQVAE-2 model, followed by the NOT-SO-BIGGAN-PIXEL model which does slightly worse than both.

Qualitative Results. For reference, we have included the FID/IS scores for a pretrained BigGAN model in Figure 3. BigGAN model records the lowest on FID and highest on IS compared to all the other models but requires an astonishing amount of compute. It takes as many as 256 TPU-v3 cores for up to 48 hours to train BigGAN on the ImageNet dataset. This is an order of magnitude larger compute than used for NOT-SO-BIGGAN that uses only 4 Tesla-V100 GPUs. Nonetheless, NOT-SO-BIGGAN is able to generate high-fidelity images across different ImageNet classes. We show some of these samples from the NOT-SO-BIGGAN model in Figure 4a. To allow for visual comparison with BigGAN, we also generate BigGAN-samples from the same subset of classes in Figure 4b. We defer the NOT-SO-BIGGAN-PIXEL samples to the Appendix E.

6 Conclusions and Future Work

In this paper, we present a new genre of scalable generative model that utilizes WT to operate in the frequency domain with a semantically meaningful low-frequency latent space. With this approach, NOT-SO-BIGGAN is not only able to generate high-fidelity class-conditional samples comparable to that of state-of-the-art, but can do so at a fraction of the compute (in both terms of resources and time). In the current version of NOT-SO-BIGGAN, we train the UNet-based decoders using MSE. However, training UNets using perceptual (or adversarial) loss could lead to further improvement in fidelity [13]. In future work, we plan to evaluate the effect of changing to this loss and to explore applications of our approach to other modalities of data, such as audio or video.

7 Broader Impact

Generative modelling of high-resolution images typically requires a high compute budget and specialized hardware, which has traditionally restricted participation of the larger research community in this field. In addition, as pointed out in [29], training large-scale neural network models, such as BigGAN, consumes enormous amounts of electricity and can result in significant environmental repercussions. As NOT-SO-BIGGAN has significantly lower compute requirements and power consumption, we hope that it can promote wider participation from the research community without significantly impacting the environment. As with any good generative model of image data, there is risk that work that builds on NOT-SO-BIGGAN could potentially be used for the creation of deliberately deceptive imagery, though we note that numerous methods for the generation of realistic fake imagery already exist and are widely available, and our method does not add anything new in terms of the quality of the synthetic imagery. We hope that our work in democratizing access to high-resolution generative models will allow us to better understand and counter potential malicious use cases that already exist.

References

- [1] A PyTorch implementation of BigGAN with pretrained weights and conversion scripts. ????. Accessed: 2020-05-30.
- [2] *Antonini Marc, Barlaud Michel, Mathieu Pierre, Daubechies Ingrid.* Image coding using wavelet transform // IEEE Transactions on image processing. 1992. 1, 2. 205–220.

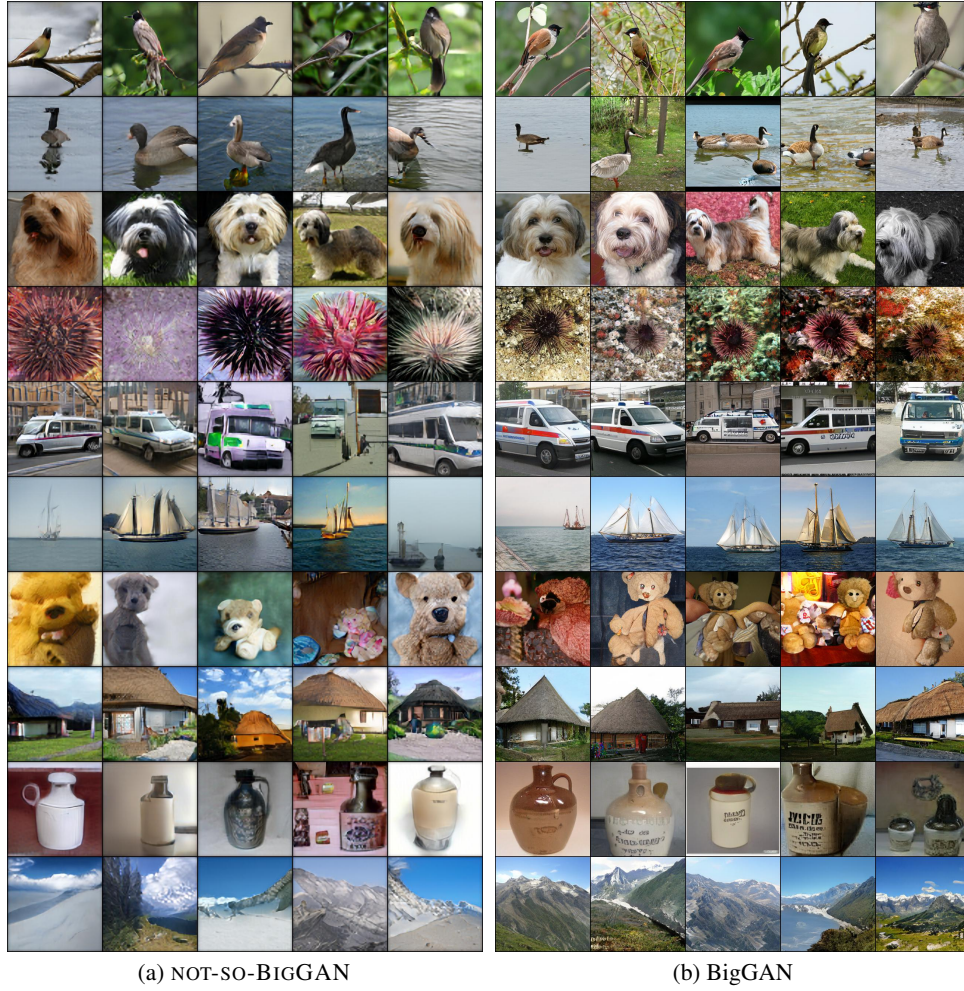


Figure 4: class-conditional random samples. Classes from the top row: 16 bulbul, 99 goose, 200 Tibetan terrier, 328 sea urchin, 734 police van, 780 schooner, 850 teddy bear, 853 thatch, 901 whiskey jug, and 970 alp.

- [3] *Arjovsky Martin, Chintala Soumith, Bottou Léon.* Wasserstein gan // arXiv preprint arXiv:1701.07875. 2017.
- [4] *Borji Ali.* Pros and cons of gan evaluation measures // Computer Vision and Image Understanding. 2019. 179. 41–65.
- [5] *Brock Andrew, Donahue Jeff, Simonyan Karen.* Large Scale GAN Training for High Fidelity Natural Image Synthesis // International Conference on Learning Representations. 2018.
- [6] *Chen Xi, Mishra Nikhil, Rohaninejad Mostafa, Abbeel Pieter.* Pixelsnail: An improved autoregressive generative model // arXiv preprint arXiv:1712.09763. 2017.
- [7] *Daubechies Ingrid.* Ten lectures on wavelets. 61. 1992.
- [8] *De Fauw Jeffrey, Dieleman Sander, Simonyan Karen.* Hierarchical autoregressive image models with auxiliary decoders // arXiv preprint arXiv:1903.04933. 2019.
- [9] *Goodfellow Ian J., Pouget-Abadie Jean, Mirza Mehdi, Xu Bing, Warde-Farley David, Ozair Sherjil, Courville Aaron C., Bengio Yoshua.* Generative Adversarial Nets // Neural Information Processing Systems. 2014.

- [10] *Gulrajani Ishaan, Ahmed Faruk, Arjovsky Martin, Dumoulin Vincent, Courville Aaron C.* Improved training of wasserstein gans // Advances in neural information processing systems. 2017. 5767–5777.
- [11] *Haar Alfred.* on the theory of orthogonal functional systems. 1909.
- [12] *Heusel Martin, Ramsauer Hubert, Unterthiner Thomas, Nessler Bernhard, Hochreiter Sepp.* GANS trained by a two time-scale update rule converge to a local nash equilibrium // Neural Information Processing Systems. 2017.
- [13] *Hu Xiaodan, Naiel Mohamed A, Wong Alexander, Lamm Mark, Fieguth Paul.* RUNet: A Robust UNet Architecture for Image Super-Resolution // Proceedings of the IEEE Conference on Computer Vision and Pattern Recognition Workshops. 2019. 0–0.
- [14] *Jouppi Norman P, Young Cliff, Patil Nishant, Patterson David, Agrawal Gaurav, Bajwa Ramin-der, Bates Sarah, Bhatia Suresh, Boden Nan, Borchers Al, others .* In-datacenter performance analysis of a tensor processing unit // Proceedings of the 44th Annual International Symposium on Computer Architecture. 2017. 1–12.
- [15] *Kingma Diederik P, Welling Max.* Auto-encoding variational bayes // arXiv preprint arXiv:1312.6114. 2013.
- [16] *Ledig Christian, Theis Lucas, Huszár Ferenc, Caballero Jose, Cunningham Andrew, Acosta Alejandro, Aitken Andrew, Tejani Alykhan, Totz Johannes, Wang Zehan, others .* Photo-realistic single image super-resolution using a generative adversarial network // Proceedings of the IEEE conference on computer vision and pattern recognition. 2017. 4681–4690.
- [17] *Li Chun-Liang, Chang Wei-Cheng, Cheng Yu, Yang Yiming, Póczos Barnabás.* Mmd gan: Towards deeper understanding of moment matching network // Advances in Neural Information Processing Systems. 2017. 2203–2213.
- [18] *Menick Jacob, Kalchbrenner Nal.* GENERATING HIGH FIDELITY IMAGES WITH SUB-SCALE PIXEL NETWORKS AND MULTIDIMENSIONAL UPSCALING // International Conference on Learning Representations. 2019.
- [19] *Mescheder Lars, Geiger Andreas, Nowozin Sebastian.* Which training methods for GANs do actually converge? // arXiv preprint arXiv:1801.04406. 2018.
- [20] *Mescheder Lars, Nowozin Sebastian, Geiger Andreas.* The numerics of gans // Advances in Neural Information Processing Systems. 2017. 1825–1835.
- [21] *Miyato Takeru, Kataoka Toshiki, Koyama Masanori, Yoshida Yuichi.* Spectral Normalization for Generative Adversarial Networks // International Conference on Learning Representations. 2018.
- [22] *Nowozin Sebastian, Cseke Botond, Tomioka Ryota.* f-gan: Training generative neural samplers using variational divergence minimization // Advances in neural information processing systems. 2016. 271–279.
- [23] *Oord Aaron van den, Vinyals Oriol, others .* Neural discrete representation learning // Advances in Neural Information Processing Systems. 2017. 6306–6315.
- [24] *Razavi Ali, Oord Aaron van den, Vinyals Oriol.* Generating diverse high-fidelity images with vq-vae-2 // Advances in Neural Information Processing Systems. 2019. 14837–14847.
- [25] *Reed Scott, Oord Aaron van den, Kalchbrenner Nal, Colmenarejo Sergio Gómez, Wang Ziyu, Chen Yutian, Belov Dan, De Freitas Nando.* Parallel multiscale autoregressive density estimation // Proceedings of the 34th International Conference on Machine Learning-Volume 70. 2017. 2912–2921.
- [26] *Ronneberger Olaf, Fischer Philipp, Brox Thomas.* U-net: Convolutional networks for biomedical image segmentation // International Conference on Medical image computing and computer-assisted intervention. 2015. 234–241.

- [27] *Roth Kevin, Lucchi Aurelien, Nowozin Sebastian, Hofmann Thomas*. Stabilizing training of generative adversarial networks through regularization // Advances in neural information processing systems. 2017. 2018–2028.
- [28] *Salimans Tim, Goodfellow Ian, Zaremba Wojciech, Cheung Vicki, Radford Alec, Chen Xi*. Improved techniques for training gans // Advances in neural information processing systems. 2016. 2234–2242.
- [29] *Schwab Katharine*. A Google intern built the AI behind these shockingly good fake images. October 2018. [Online; posted 10-02-18].
- [30] *Srivastava Akash, Valkov Lazar, Russell Chris, Gutmann Michael U, Sutton Charles*. Veegan: Reducing mode collapse in gans using implicit variational learning // Advances in Neural Information Processing Systems. 2017. 3308–3318.
- [31] *Srivastava Akash, Xu Kai, Gutmann Michael U., Sutton Charles*. Generative Ratio Matching Networks // International Conference on Learning Representations. 2020.
- [32] *Wang Xintao, Yu Ke, Wu Shixiang, Gu Jinjin, Liu Yihao, Dong Chao, Qiao Yu, Change Loy Chen*. Esrgan: Enhanced super-resolution generative adversarial networks // Proceedings of the European Conference on Computer Vision (ECCV). 2018. 0–0.
- [33] *Zhang Han, Goodfellow Ian, Metaxas Dimitris, Odena Augustus*. Self-attention generative adversarial networks // arXiv preprint arXiv:1805.08318. 2018.
- [34] *Zhao Yang, Li Chunyuan, Yu Ping, Gao Jianfeng, Chen Changyou*. Feature Quantization Improves GAN Training // arXiv preprint arXiv:2004.02088. 2020.

A Slicing

Figure 5b, shows the difference between the slicing operations of SPN and NOT-SO-BIGGAN. SPN slices the images across the spatial dimensions thus introducing long-term dependencies. In contrast, NOT-SO-BIGGAN decomposes the image along different frequency bands that preserves the global structure of the image in each of the patches.

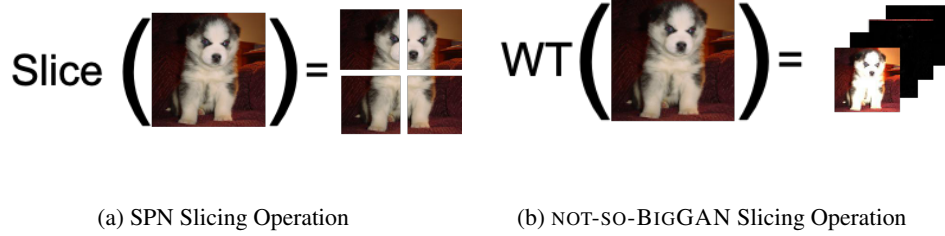


Figure 5: Unlike SPN, NOT-SO-BIGGAN slices the images in the frequency domain. As a result each patch contains the entire global structure of the input image. This helps alleviate any long-term dependency issues.

B Architecture and Hyperparameters

B.1 Sampler

	NOT-SO-BIGGAN	NOT-SO-BIGGAN-PIXEL
Best model type	BigGAN-deep	BigGAN
Batch size	512	512
Learning rate of generator	1e-4	1e-4
Learning rate of discriminator	4e-4	4e-4
Attention resolution	128	120
Dimension of random noise (z dim)	32	32
Number of resblocks per stage in generator/discriminator	2	1
Adam optimizer β_1	0	0
Adam optimizer β_2	0.999	0.999
Adam optimizer ϵ	1e-8	1e-8
Training iterations	250000	250000

Table 2: Hyperparameters of NOT-SO-BIGGAN samplers (wavelet and pixel)

B.2 NOT-SO-BIGGAN Decoders

Refer to Figure 6a and Table 3 for architecture details and hyperparameters of NOT-SO-BIGGAN decoders.

B.3 NOT-SO-BIGGAN-PIXEL Decoders

Refer to Figure 6b and Table 4 for architecture details and hyperparameters of NOT-SO-BIGGAN-PIXEL decoders.

	Level 1 Decoder	Level 2 Decoder
Input size	32×32	32×32
Batch size	128	64
Learning rate	1e-4	1e-4
Layers	16	16
Conv filter size	3	3
Number of added shallow networks	12	48
Adam optimizer β_1	0.9	0.9
Adam optimizer β_2	0.999	0.999
Adam optimizer ϵ	1e-8	1e-8
Training iterations	288000	232000

Table 3: Hyperparameters of NOT-SO-BIGGAN decoders (level 1 and level 2)

	Level 1 Decoder	Level 2 Decoder
Input size	64×64	128×128
Batch size	64	64
Learning rate	1e-4	1e-4
Layers	19	19
Conv filter size	3	3
Adam optimizer β_1	0.9	0.9
Adam optimizer β_2	0.999	0.999
Adam optimizer ϵ	1e-8	1e-8
Training iterations	615000	178000

Table 4: Hyperparameters of NOT-SO-BIGGAN-PIXEL decoders (level 1 and level 2)

C NOT-SO-BIGGAN vs NOT-SO-BIGGAN-PIXEL Information Content

As we show in Figure 7, the information content in the latent embedding of NOT-SO-BIGGAN and NOT-SO-BIGGAN-PIXEL are drastically different. The TL patches from NOT-SO-BIGGAN preserve more information about the encoded image than the downsampled image from NOT-SO-BIGGAN-PIXEL, therefore leading to better deterministic reconstructions. Also, unlike NOT-SO-BIGGAN decoder that circumvents the CoD by avoiding any reconstructions in the original dimensionality, the NOT-SO-BIGGAN-PIXEL decoder still has to operate on the full image size, resulting in a larger model.

D Additional NOT-SO-BIGGAN Samples

Refer to Figure 8 for additional samples from NOT-SO-BIGGAN.

E NOT-SO-BIGGAN-PIXEL Samples

Refer to Figure 9a for class-conditional random samples from NOT-SO-BIGGAN-PIXEL. Samples from BigGAN are also included in 9b for comparison.

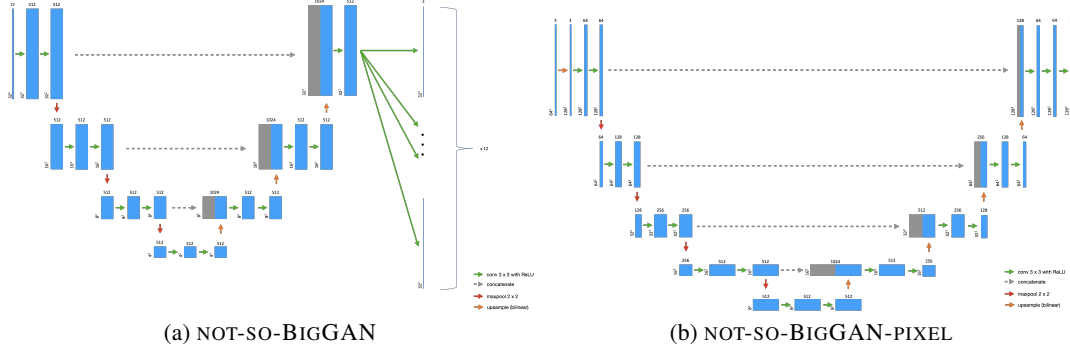


Figure 6: UNet-based decoding architecture for NOT-SO-BIGGAN and NOT-SO-BIGGAN-PIXEL models.

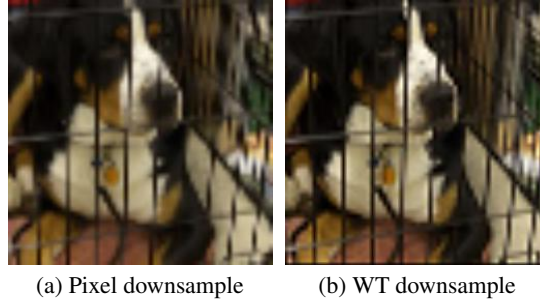


Figure 7: (a) and (b) are downsampled versions of the same image using bilinear interpolation and wavelet transformation, respectively.

F Full Resolution Samples from NOT-SO-BIGGAN

Refer to Figures 10, 11, 12, and 13 for full resolution samples from NOT-SO-BIGGAN.

G Full Resolution Samples from NOT-SO-BIGGAN-PIXEL

Refer to Figures 14, 15, 16, and 17 for full resolution samples from NOT-SO-BIGGAN-PIXEL.

H Power Usage

Our NOT-SO-BIGGAN model takes 70.56 kWh to train. In comparison, the BigGAN model has several orders of magnitude higher energy requirement.

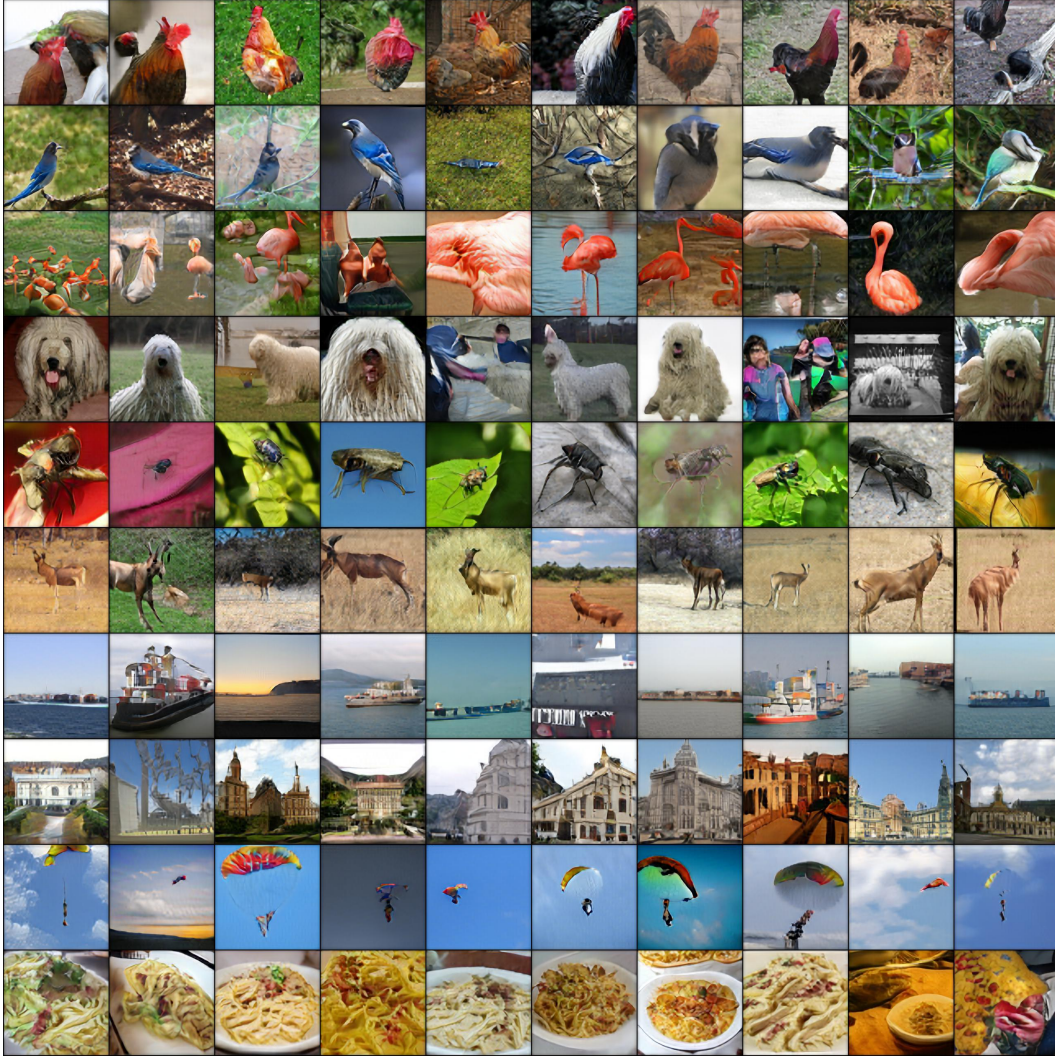


Figure 8: Additional class-conditional random samples from NOT-SO-BIGGAN. Classes from the top row: 7 cock, 17 jay, 130 flamingo, 142 dowitcher, 228 komondor, 308 fly, 351 hartebeest, 510 container ship, 698 palace, 701 parachute, and 959 carbonara.



Figure 9: Class-conditional random samples. Classes from the top row: 0 *Tinca tinca*, 1 goldfish, 139 ruddy turnstone, 143 oyster catcher, 323 monarch butterfly, 386 African elephant, 493 chiffonier, 780 schooner, 946 cardoon, and 992 agaric.

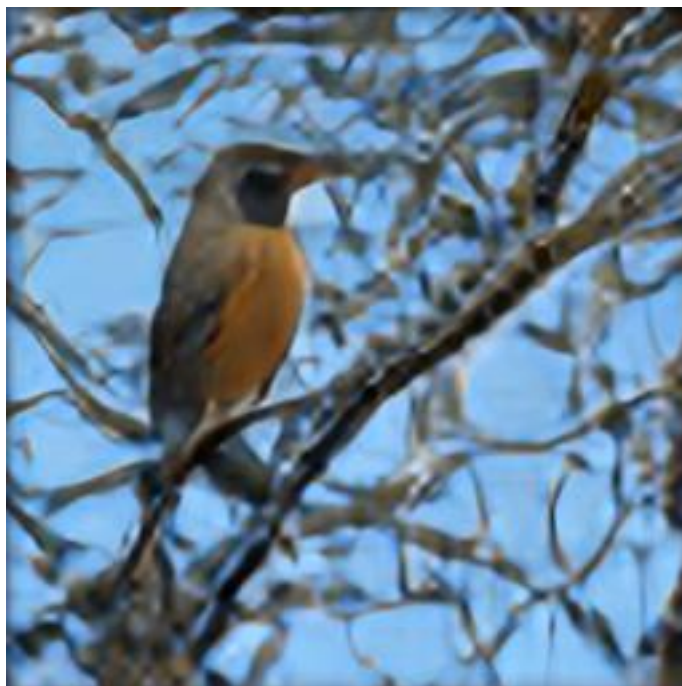


Figure 10: Full resolution sample from NOT-SO-BIGGAN.

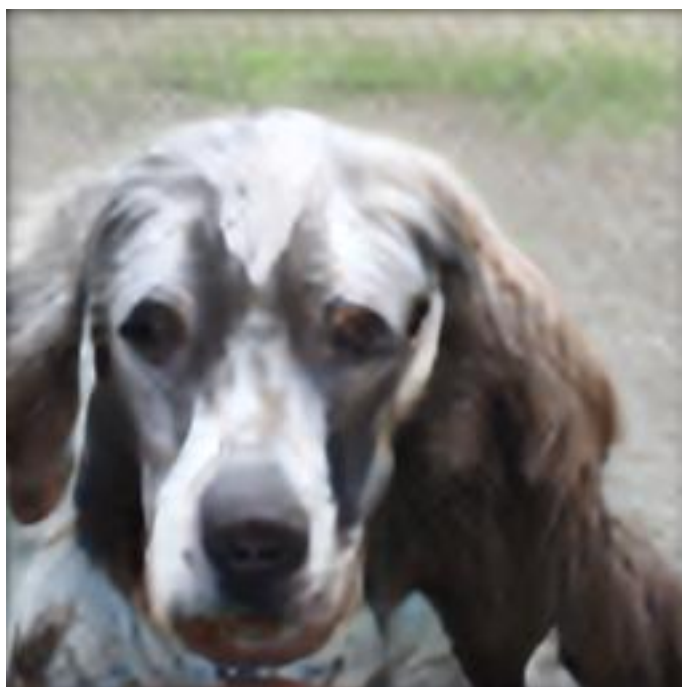


Figure 11: Full resolution sample from NOT-SO-BIGGAN.



Figure 12: Full resolution sample from NOT-SO-BIGGAN.



Figure 13: Full resolution sample from NOT-SO-BIGGAN.



Figure 14: Full resolution sample from NOT-SO-BIGGAN-PIXEL.

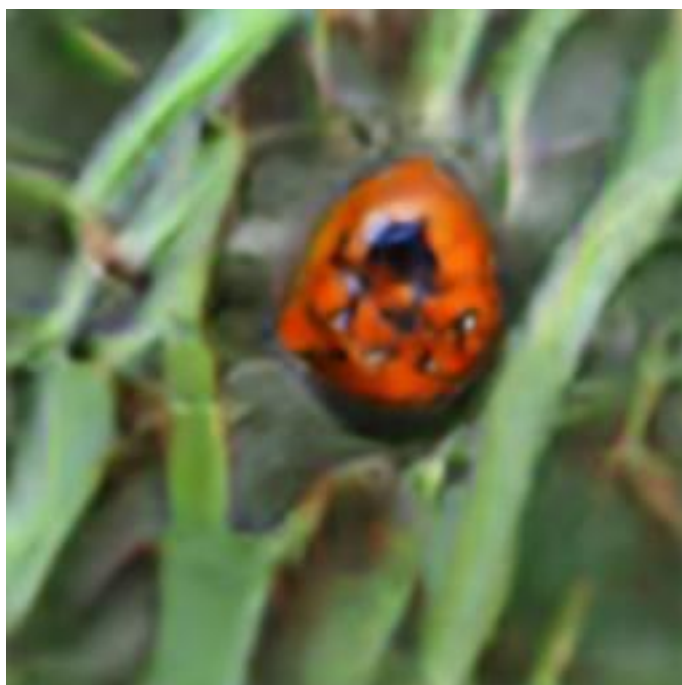


Figure 15: Full resolution sample from NOT-SO-BIGGAN-PIXEL.



Figure 16: Full resolution sample from NOT-SO-BIGGAN-PIXEL.

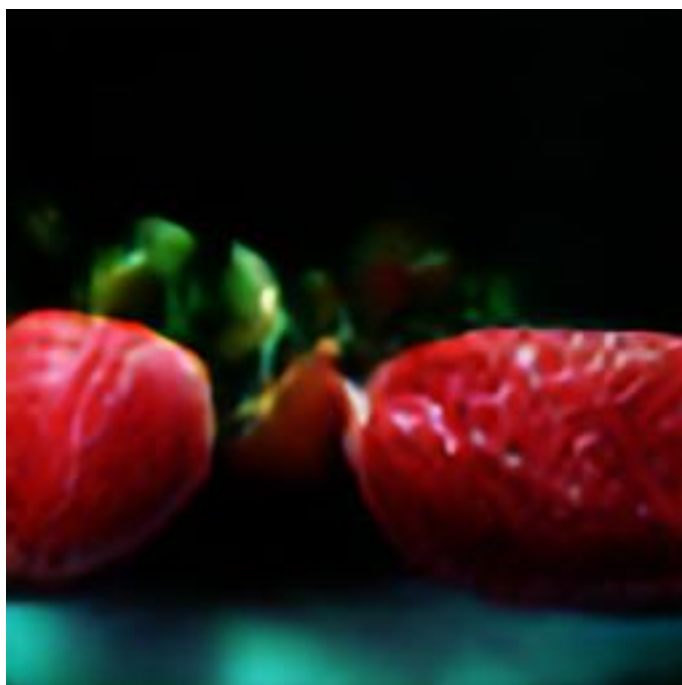


Figure 17: Full resolution sample from NOT-SO-BIGGAN-PIXEL.